CrystEngComm

Cite this: *CrystEngComm*, 2012, **14**, 5905–5913

www.rsc.org/crystengcomm

PAPER

Two 3D metal–organic frameworks with different topologies, thermal stabilities and magnetic properties†

Ting Gao,[a] Xiao-Zhu Wang,[a] Hao-Xue Gu,[a] Yan Xu,[a] Xuan Shen[a] and Dun-Ru Zhu*[ab]

Received 28th March 2012, Accepted 31st May 2012
DOI: 10.1039/c2ce25442e

Two novel 3D metal–organic frameworks, $[ML]_n$ (M = Co, **1**; Mn, **2**) were successfully prepared in solvothermal conditions using 3,3′-dimethoxy-4,4′-biphenyldicarboxylic acid (H_2L) as the ligand. X-Ray crystallography analysis reveals that MOF **1** crystallizes in the monoclinic system, space group $P2_1/c$ in contrast to MOF **2** in the tetragonal system, space group $I\bar{4}$. MOF **1** contains an elongated $[CoO_6]$ octahedron with two bound methoxy groups in the *trans* position, whereas MOF **2** has a compressed $[MnO_6]$ octahedron with two coordinated methoxy groups in the *cis* arrangement. The ligand L shows a novel bis(tridentate) bridging coordination mode. MOF **1** exhibits a 3D framework with $CdSO_4$ (**cds**) topology consisting of two different nodes and good thermal stability (313 °C). MOF **2** is a doubly interpenetrated 3D α-Po framework with a higher thermal stability (368 °C). The study of magnetic properties in the temperature range of 1.8–300 K shows the occurrence of weak ferromagnetic interactions (J = 0.15 K) between the high-spin Co(II) ions in **1**, but a weak antiferromagnetic coupling ($J = -0.15$ cm^{-1}) between Mn(II) ions in **2** due to the *syn-anti* carboxylate bridge.

Introduction

The rational design and construction of metal–organic frameworks (MOFs) based upon the assembly of metal ions and multifunctional organic ligands is an interesting research field. This not only stems from their intriguing structural topologies but also from their potential application as functional materials.[1,2] An effective and facile approach for the synthesis of MOFs is still based on the appropriate choice of well-designed organic ligands as bridges. Among the various ligands, rigid multicarboxylic acids such as 1,4-benzenedicarboxylic acid (H_2BDC),[3] 1,3,5-benzenetricarboxylic acid (H_3BTC),[4] and 4,4′-biphenyldicarboxylic acid (H_2BPDC),[5] have been extensively employed in the preparation of MOFs. However, substituted aromatic multicarboxylic acids remain largely unexplored.[6]

In our previous work,[7] a symmetrically substituted ligand: 3,3′-dimethoxy-4,4′-biphenyldicarboxylic acid (H_2L) was successfully used to construct MOFs with transition metal ions [Cd(II), Zn(II), Cu(II)] and lanthanide ions [Eu(III), Gd(III), Dy(III)]. It was also found that the ligand L could adopt four types of different coordination modes (Scheme 1). Moreover, the attachment of two methoxy groups on the H_2BPDC could not only provide additional coordinating sites and produce intriguing structural topologies, but could also create more robust networks with high thermal stabilities. As a continuation of our investigation of MOFs based on H_2L, herein we report the syntheses of two novel 3D MOFs, $[CoL]_n$ (**1**) and $[MnL]_n$ (**2**). Their single crystal structures, spectral properties, thermal stabilities, and magnetic properties are systematically investigated. In addition, a novel coordination mode of the ligand L is also observed.

Experimental section

Materials and methods

The reagents were obtained from commercial sources and used without further purification. 3,3′-dimethoxy-4,4′-biphenyldicarboxylic acid (H_2L) was prepared according to our method.[7] Elemental analyses (C, H) were carried out with a Thermo Finnigan Flash 1112A elemental analyzer. IR spectra were recorded in the range 4000–400 cm^{-1} using KBr pellets on a Nicolet Avatar 380 FT-IR spectrophotometer. Thermogravimetric analyses (TGA) were performed on a NETZSCH STA 449C thermal analyzer under nitrogen atmosphere at a heating rate of 10 °C min^{-1}. Powder X-ray diffraction (PXRD) data were collected on a Bruker D8 Advance diffractometer with Cu-Kα radiation (λ = 1.5406 Å). Temperature-dependent magnetic measurements were carried out on a Quantum Design MPMS-7 SQUID magnetometer. Diamagnetic corrections were made with Pascal's constants.[8]

[a]*State Key Laboratory of Materials-Oriented Chemical Engineering, College of Chemistry and Chemical Engineering, Nanjing University of Technology, Nanjing, 210009, P. R. China*
[b]*State Key Laboratory of Coordination Chemistry, Nanjing University, Nanjing, 210093, P. R. China. E-mail: zhudr@njut.edu.cn; Fax: 86 25 83172261.; Tel: 86 25 83587717*

† Electronic supplementary information (ESI) available: Molecular structures, IR spectra, and simulated and experimental P-XRD patterns of **1** and **2**. CCDC reference numbers 870789 (**1**) and 870790 (**2**). For ESI and crystallographic data in CIF or other electronic format see DOI: 10.1039/c2ce25442e

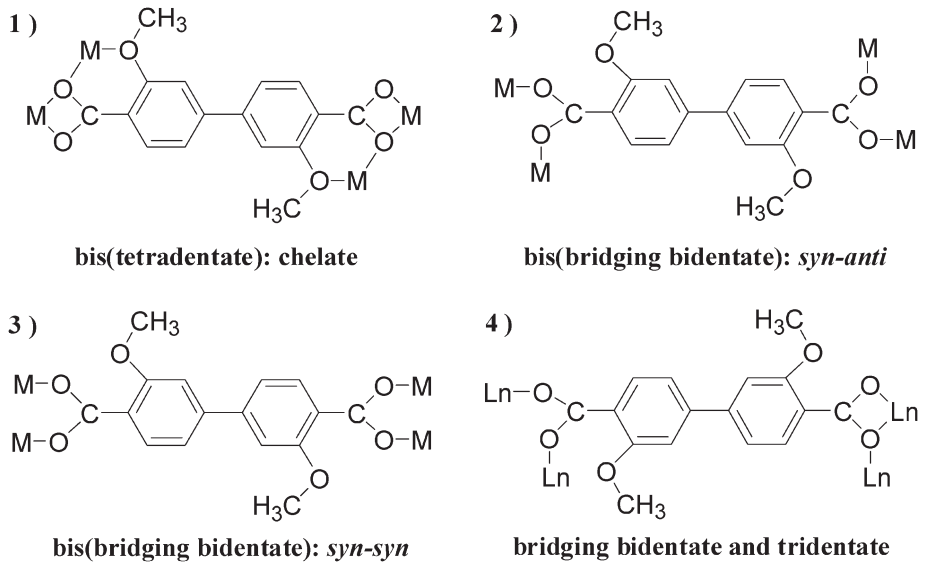

Scheme 1 The known coordination modes of ligand L from previous work.[7]

Synthesis of $[CoL]_n$ (1)

A mixture of $CoCl_2{\cdot}6H_2O$ (0.0241 g, 0.1 mmol) and H_2L (0.0304 g, 0.1 mmol) in mixed solvent DMF/MeOH/H_2O (0.6 mL/0.6 mL/0.6 mL) was heated in a 25 mL capacity stainless-steel reactor lined with Teflon at 120 °C for 2 days and then cooled to room temperature. Amaranthine block crystals of **1** were obtained. Yield, 87.4% (0.0314 g) based on the ligand. IR (cm^{-1}): 3079(w), 3038(w), 2951(w), 1592(vs), 1544(s), 1484(m), 1399(vs), 1374(vs), 1229(s), 1125(m), 1013(s), 860(s), 780(s), 673(m). Anal. calcd for $C_{16}H_{12}CoO_6$: C, 53.50; H, 3.37. Found: C, 53.41; H, 3.49.

Synthesis of $[MnL]_n$ (2)

This MOF was obtained following the same method as for **1** except by replacing $CoCl_2{\cdot}6H_2O$ with $MnCl_2{\cdot}4H_2O$. Light yellow octahedral crystals of **2** were obtained. Yield, 65.6% (0.0233 g) based on the ligand. IR (cm^{-1}): 3062(w), 2940(w), 1651(s), 1593(vs), 1562(s), 1448(s), 1408(vs), 1373(s), 1224(s), 1184(s), 1115(m), 1004(s), 852(s), 782(s), 671(m). Anal. calcd for $C_{16}H_{12}O_6Mn$: C, 54.10; H, 3.41. Found: C, 54.26; H, 3.57.

X-Ray crystallography

Diffraction data for **1** and **2** were collected on a Bruker Smart APEX II CCD diffractometer with graphite-monochromated Mo-Kα radiation (λ = 0.71073 Å). Empirical absorption corrections were applied by using the SADABS program. The structures were solved by direct methods and refined by the full-matrix least-squares method based on F^2 using the SHELXTL-97 program.[9] All non-hydrogen atoms were refined anisotropically. Atoms C2–C10, C12 and C13 in MOF **2** were found to be disordered over two positions and fixed at 0.5. The hydrogen atoms in MOF **1** were placed on calculated positions and assigned isotropic thermal parameters riding on their parent atoms. The hydrogen atoms in MOF **2** could not be located and were not calculated due to the disorder of the parent atoms. The crystal data and structural refinements of MOFs **1** and **2** are summarized in Table 1. Selected bond lengths and angles of MOFs **1** and **2** are listed in Table 2.

Results and discussion

Crystal structure of 1

Single-crystal X-ray analysis reveals that **1** crystallizes in the monoclinic system, space group $P2_1/c$ and the asymmetric unit consists of 0.5 of a Co^{2+} ion and 0.5 of a L ligand (Fig. S1a in ESI†). As shown in Fig. 1a, each Co^{2+} ion is coordinated by four equatorial carboxyl oxygen atoms from four different L ligands and two axial oxygen atoms from methoxy groups [O3 and O3A] to form an elongated [CoO_6] octahedron (Fig. 1c). The adjacent octahedra exhibit a tilt angle of 54.73(11)° between their respective long axes (O3···O3A) along each Co(II)–O–C–O–Co(II) pathway (Fig. 2a). Each L ligand coordinates to four Co^{2+} ions in a bis(bridging tridentate) mode (Scheme 2). The Co1–O3 bond length is 2.173(3) Å, similar to those found in the Co^{2+}

Table 1 Crystal data and structural refinements for MOFs **1** and **2**

MOFs	1	2
Empirical formula	$C_{16}H_{12}CoO_6$	$C_{16}H_{12}MnO_6$
Formula weight	359.19	355.20
Crystal system	Monoclinic	Tetragonal
Space group	$P2_1/c$	$I\bar{4}$
a/Å	12.028(3)	7.7455(14)
b/Å	6.7017(19)	7.7455(14)
c/Å	8.628(3)	24.912(9)
β (°)	97.218(4)	90.00
V/Å^3	690.0(3)	1494.5(7)
Z	2	4
ρ_c/g cm^{-3}	1.729	1.525
μ/mm^{-1}	1.274	0.912
F(000)	366	676
Reflection collected	1173	1400
Unique reflections	872	1267
GOF on F^2	1.055	1.083
R_1, wR_2 [$I > 2\sigma(I)$]	0.0398/0.0972	0.0483/0.1272
R_1, wR_2 (all data)	0.0596/0.1369	0.0556/0.1330

Table 2 Selected bond lengths (Å) and angles (°) for MOFs **1** and **2**[a]

1			
Co1–O1	2.019(3)	Co1–O2^{i}	2.068(3)
Co1–O3	2.173(3)	Co1···Co1A	5.462(3)
Co1···Co1C	8.628(3)	Co1A···Co1B	6.702(3)
O1–Co1–O2^{i}	91.05(13)	O1–Co1–O3	83.14(11)
O1–Co1–O3^{iii}	96.86(11)	O2^{i}–Co1–O3	96.19(11)
O2^{ii}–Co1–O3	83.82(11)	O3^{iii}–Co1–O3	180.000(1)
2			
Mn1–O2	2.108(3)	Mn1–O1^{iv}	2.050(3)
Mn1–O3^{iv}	2.418(3)	Mn1···Mn1A	5.490(3)
Mn1A···Mn1B	7.746(3)		
O1^{iv}–Mn1–O2	98.64(11)	O1^{iv}–Mn1–O3^{vi}	81.05(12)
O2–Mn1–O2^{v}	83.99(11)	O1^{vi}–Mn1–O2	98.74(11)
O3^{iv}–Mn1–O3^{vi}	75.89(12)	O1^{iv}–Mn1–O3^{iv}	80.49(12)
O2–Mn1–O3^{iv}	175.93(11)	O1^{iv}–Mn1–O1^{vi}	156.53(9)

[a] Symmetry codes: i) 2 − *x*, −1/2 + *y*, 3/2 − *z*; ii) *x*, 1/2 − *y*, 1/2 + *z*; iii) 2 − *x*, −*y*, 2 − *z*, iv) −1 + *y*, 1 − *x*, −*z*; v) −*x*, 1 − *y*, *z*; vi) 1 − *y*, *x*, −*z*.

complexes with methoxy coordination.[10] The Co–O(CO_2^-) bond distances are in the range of 2.019(3) to 2.068(3) Å. Each Co^{2+} ion is simultaneously bridged to four adjacent Co^{2+} ions by the carboxylic groups in a *syn-anti* conformation, forming a 16-membered $Co_4(CO_2)_4$ rhombic ring with a Co···Co distance of 5.462(3) Å at one side (Fig. 3a), which is longer than those found in the similar Co(II) complexes.[11,19b,c] The dimensions of the rhombus estimated by two diagonal Co···Co distances and two vertex angles ∠Co···Co···Co have been shown in Table 3. These rhombuses treated topologically as a 4-connected node are repeatedly interconnected to produce a 2D network located exactly in the *bc* plane (Fig. 3a). These 2D networks are further connected by the biphenyl groups of ligand L along the *a* axis to generate a 3D framework (Fig. 3b). If the symmetric center of ligand L is treated as another node, the 3D framework of MOF **1** can be regarded topologically as a $CdSO_4$ (**cds**) net (Fig. 3c). Although many Co^{2+} complexes with **cds** topology have been reported,[12] the known examples are often composed of only one node [Co^{2+} ion], which is prominently different from that observed in MOF **1** whose **cds** topology consists of two different nodes [Co^{2+} ion and L_{center}]. Notably, there is a strong intermolecular edge-to-face C–H···π interaction involving C3–H3A and one phenyl ring (C2–C7)^{i} of the biphenyl groups (H3A···π^{i} = 3.07 Å and ∠C3–H3A···π^{i} = 131°, i: *x*, 1/2 − *y*, *z* − 1/2) (Fig. 4), which is helpful to stabilize the 3D framework.

Crystal structure of 2

Different from **1**, MOF **2** crystallizes in the tetragonal system, space group $I\bar{4}$ and the asymmetric unit consists of 0.5 of a Mn^{2+} ion and 0.5 of a L ligand (Fig. S1b in ESI†). Although the Mn(II) center is also six coordinated by four carboxyl oxygen atoms from four different L ligands and two oxygen atoms from methoxy groups [O3 and O3A], the O3 and O3A atoms are located at a *cis*-position in the equatorial plane (Fig. 1b) and the [MnO_6] core is a severely distorted compressed octahedron (Fig. 1d, Table 2). The adjacent octahedra exhibit a tilt angle of 11.72(11)° between their respective short axes (O1···O1A) along each Mn(II)–O–C–O–Mn(II) pathway (Fig. 2b). The Mn1–O3 bond length is 2.418(3) Å, which is longer than those found in Mn(II) complexes with bound methoxy groups.[13] The Mn–O(CO_2^-) bond distances are in the range of 2.050(3)–2.108(3) Å, similar to those observed in the related Mn(II) carboxylate complexes.[4d,14] Each carboxylic group bridges two adjacent Mn^{2+} ions in a *syn-anti* mode to form a 16-membered $Mn_4(CO_2)_4$ square with a Mn···Mn distance of 5.490(3) Å (Fig. 5a). The diagonal Mn···Mn distance in the square is 7.746 Å (Table 3). These squares as a 4-connected node topologically are repeatedly linked to form a 2D network in the *ab* plane though the Mn1 ion has the maximum displacement of 0.377(3) Å from the plane (Fig. 5a). These 2D networks are further connected by the biphenyl groups of ligand L along the *c* axis to produce a 3D framework (Fig. 5b). This 3D framework can be treated topologically as a two fold interpenetrated α-Po net as shown in Fig. 5c.

The coordination mode of the ligand

Organic polycarboxylates have been widely employed to prepare MOFs partly due to their diverse coordination modes. In **1** and **2** all carboxyl groups of the ligand H_2L are deprotonated and the

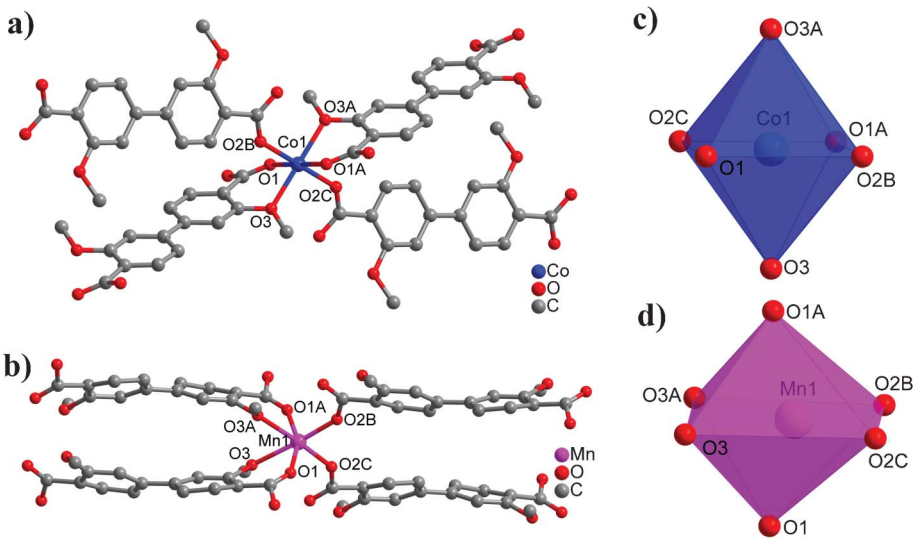

Fig. 1 The coordination environment of M^{2+} in MOFs **1** (a, c; M = Co^{2+}) and **2** (b, d; M = Mn^{2+}).

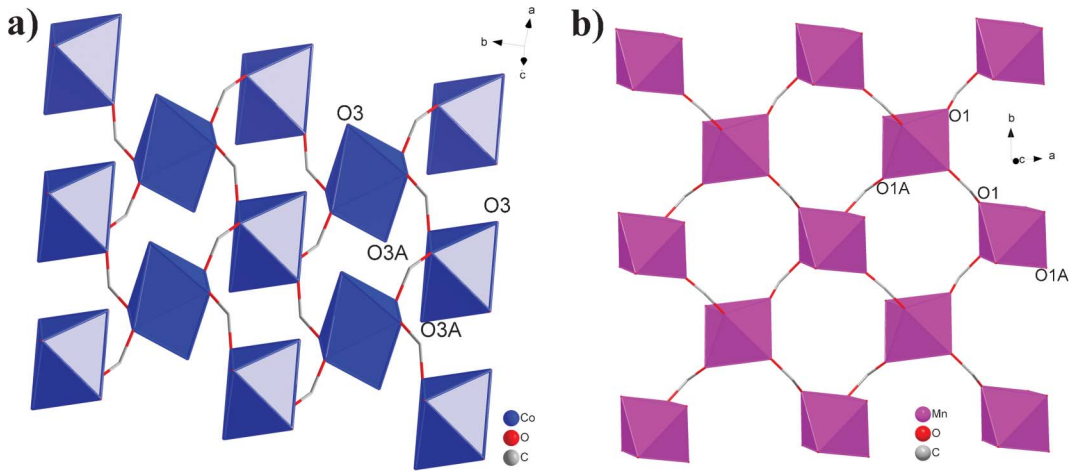

Fig. 2 Perspective view of the planar arrangement of the M(II) atoms at the centre of oxygen octahedra with *syn-anti* carboxylato bridges (the H atoms are omitted for clarity). (a) $Co_4(CO_2)_4$ rhombuses in **1**; (b) $Mn_4(CO_2)_4$ squares in **2**.

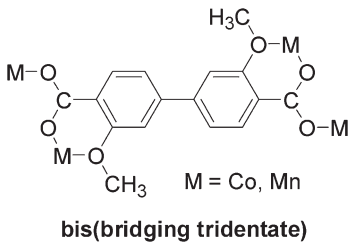

Scheme 2 A novel coordination mode of ligand L in MOFs **1** and **2**.

ligand L adopts a novel coordination mode. As shown in Scheme 2, each ligand L can link three M(II) ions in an unusual bis(tridentate) coordination mode with the help of coordinated methoxy groups, which is prominently different from those observed in our previous work (Scheme 1).[7] Moreover, the two methoxy groups are in the *trans* position in **1** but in the *cis* arrangement in **2** (Fig. 1c and 1d). Although the two methoxy groups are located in a *trans* conformation relative to the biphenyl rings, they can affect the conformation of the biphenyl rings in **1** and **2** to some extent. In fact, the biphenyl rings are coplanar in **1** but there is a dihedral angle of 29.8(1)° in **2**. There are distinct dihedral angles between the carboxylate groups and the phenyl rings in **1** [25.9(1)°] and **2** [31.4(1)° and 32.3(1)°]

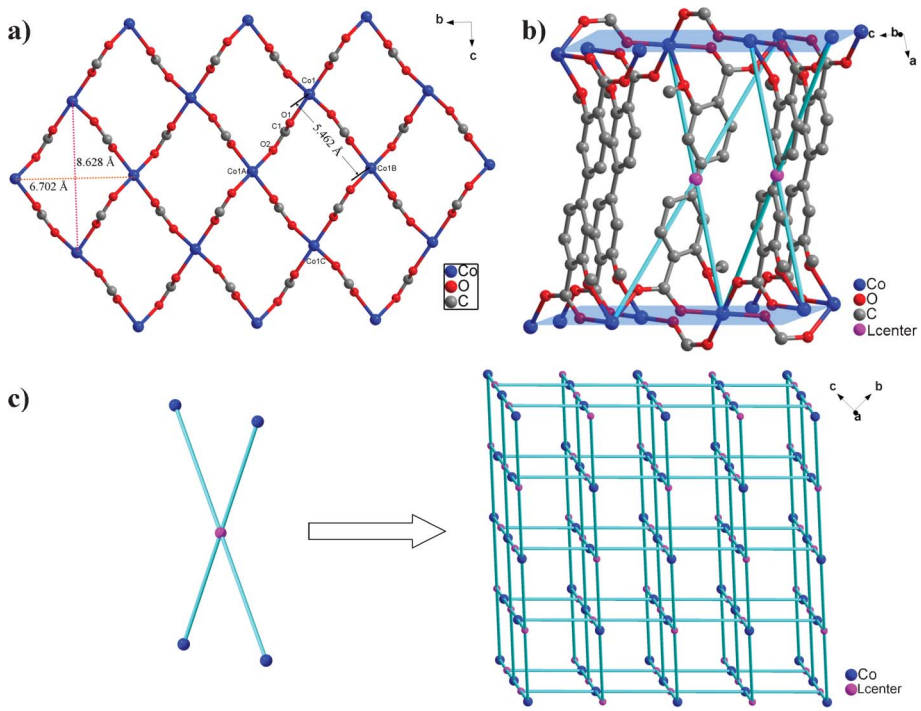

Fig. 3 The crystal structure of **1** (all hydrogen atoms are omitted for clarity). (a) (4, 4) net and $Co_4(CO_2)_4$ rhombic rings. (b) 3D framework of **1**. (c) Schematic view of the **cds** network; sky blue spheres and green lines represent Co^{2+} ions and L ligands, respectively.

Table 3 Comparison of the detailed structures for MOFs **1** and **2**

MOF	3D net	SBU	CH_3O Group	$M_4(CO_2)_4$		Dihedral angle (°)	
				M···M distance (Å)	angle (°)	Ph/Ph rings	CO_2^{2-}/Ph ring
1	**cds**	CoO_6	*trans*	6.702, 8.628	104.3, 75.7	0	25.9
2	α-Po	MnO_6	*cis*	7.746	89.7	29.8	31.4, 32.3

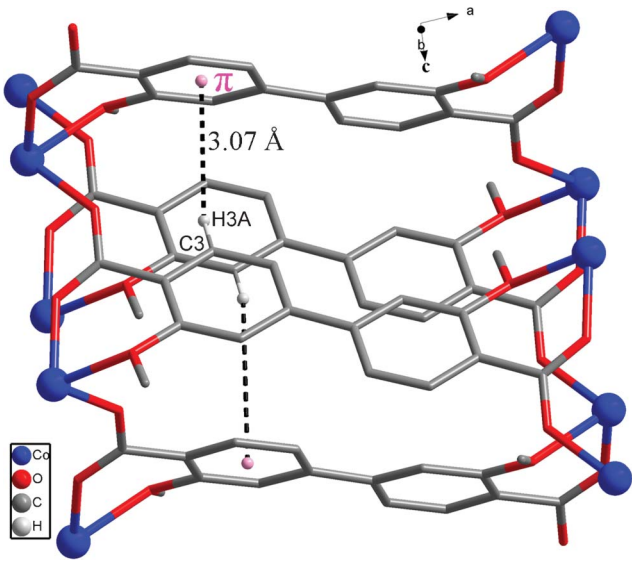

Fig. 4 The intermolecular edge-to-face C–H···π interaction in **1**.

(Table 3). Therefore, we think that it is the unique coordination mode and different conformation of the ligand that are responsible for the structure of the frameworks, the intermolecular edge-to-face C–H···π interactions and the stability (see following TG analysis) in MOFs **1** and **2**.

IR spectra

IR spectra of **1** and **2** display the characteristic asymmetric (ν_{as}) and symmetric (ν_s) stretching vibrations of carboxylate groups (see Fig. S2a and S2b in ESI†). The difference between ν_{as} and ν_s ($\Delta = \nu_{as} - \nu_s$) has been widely used as a diagnosis of the coordination mode of the carboxylate group. Generally, the monodentate carboxylate exhibits a much larger Δ value than the chelating one, and the value for the bridging mode is intermediate.[15] In **1** and **2**, the ν_{as}(COO) vibrations appear at 1592 cm^{-1} and 1651 cm^{-1}, and ν_s(COO) vibrations appear at 1399 cm^{-1} and 1448 cm^{-1}. The intermediate Δ value [193 cm^{-1} (**1**); 203 cm^{-1} (**2**)] is consistent with the bridging coordination of the group, as revealed by the X-ray diffraction analyses.

P-XRD and TG analyses

The simulated and experimental P-XRD patterns of **1** and **2** are shown in Fig. S3 and S4 (ESI†), respectively. Their peak

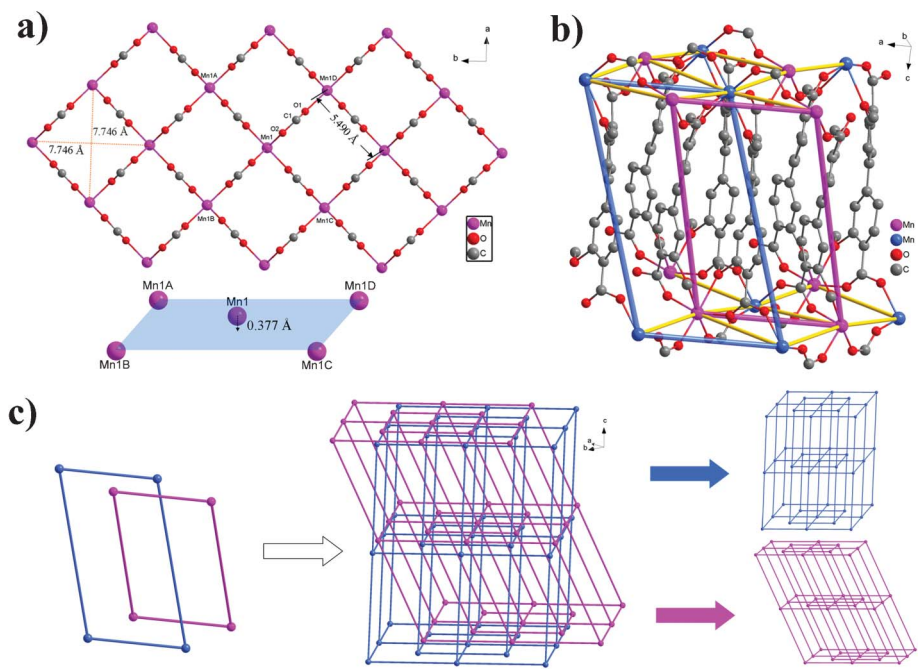

Fig. 5 The crystal structure of **2** (all hydrogen atoms are omitted for clarity). (a) (4, 4) net and $Mn_4(CO_2)_4$ squares. (b) 3D framework of **2**. (c) Schematic view of a two fold interpenetrated α-Po net: the sphere and line represent Mn^{2+} ions and L ligands, respectively; blue and red represent different α-Po nets.

positions are in good agreement with each other indicating the phase purity of the bulk products.

TGA shows high thermal stabilities of both **1** and **2** because no guest molecules are present in the structures. For **1** and **2**, an abrupt weight loss was only observed above 313 and 368 °C, respectively, due to the decomposition of the frameworks (Fig. 6). The thermal stability of **1** is higher than those found for related Co(II) complexes with BPDC ligands, $\{[Co(BPDC)(bpdap)]\cdot 1.5H_2O\}_n$ and $[Co(BPDC)(Hpb)(H_2O)]_n$ [bpdap = *N*,*N*′-bis(2-pyridyl)-2,6-diaminopyridine and Hpb = 2-(2-pyridyl)benzinidazole],[16] whose frameworks decomposed at 275 and 265 °C, respectively. The coordination network of **2** is more robust than that of a related Mn(II) MOF $[Mn(PIP)_2(BPDC)(H_2O)]\cdot 2H_2O$ (PIP = 2-phenylimidazo[4,5-*f*]1,10-phenanthroline) decomposed at 301 °C.[17] The high thermal stabilities of **1** and **2** can be explained by two factors: (1) The substituted methoxy groups may have a space-filling effect on the framework structure. (2) The involvement of the oxygen atoms from the methoxy groups in the coordination to the metal centers further strengthens the framework stability. This situation has been observed in a similar Cd(II) MOF.[7] In addition, the unique two fold interpenetrated framework also contributes to the higher thermal stability of **2**.

Magnetic properties of 1

The magnetic susceptibilities of **1** were measured in the temperature range from 1.8 to 300 K under a 2000 Oe field. The plots of χ_M and χ_M^{-1} (χ_M being the molar magnetic susceptibility per Co(II) ion) *vs.* *T* are shown in Fig. 7a. Upon cooling down, χ_M increases continuously up to a maximum of 1.47 $cm^3\ mol^{-1}$ at 1.8 K. The χ_M^{-1} *vs.* *T* plot shows a linear dependence with the temperature in the high temperature regime ($T > 150$ K), and the data follow the Curie–Weiss law well ($\chi_M = C/(T - \theta)$) with $C = 3.22\ cm^3\ K\ mol^{-1}$ and $\theta = -14.3$ K. The value of the Curie constant is consistent with the presence of hexacoordinated high-spin Co(II) ions (C = 2.8–3.4 $cm^3\ K\ mol^{-1}$)[18] and the negative sign of the Weiss temperature suggests phenomenologically the occurrence of antiferromagnetic exchange interactions. The plot of $\chi_M T$ *vs.* *T* is shown in Fig. 7b. At 300 K the value of $\chi_M T$ is equal to 3.06 $cm^3\ K\ mol^{-1}$, which is larger than the spin-only value of 1.87 $cm^3\ K\ mol^{-1}$ expected for a high-spin Co(II) ion ($S = 3/2$, $g = 2$), in accordance with the well-documented orbital angular momentum contribution of the octahedral Co(II) ion with a $^4T_{1g}$ ground state at high temperature.[18] With decreasing temperature, the $\chi_M T$ value decreases smoothly to a value of 2.78 $cm^3\ K\ mol^{-1}$ at 90 K, then sharply to reach a minimum of 2.13 $cm^3\ K\ mol^{-1}$ at 8 K. This result is well understood from the spin-orbit coupling effect for octahedral Co(II) ions.[18] As well known, a minimum value of $\chi_M T \approx 1.8\ cm^3\ K\ mol^{-1}$ is expected for isolated octahedral Co(II) ions at low temperature corresponding to a *pseudo*-spin $S = 1/2$ and $g \approx 4.4$.[19] Below 8 K, the $\chi_M T$ value increases abruptly up to 2.65 $cm^3\ K\ mol^{-1}$ at 1.8 K, suggesting the existence of ferromagnetic correlations, in agreement with the data reported by Rabu *et al.*[19b]

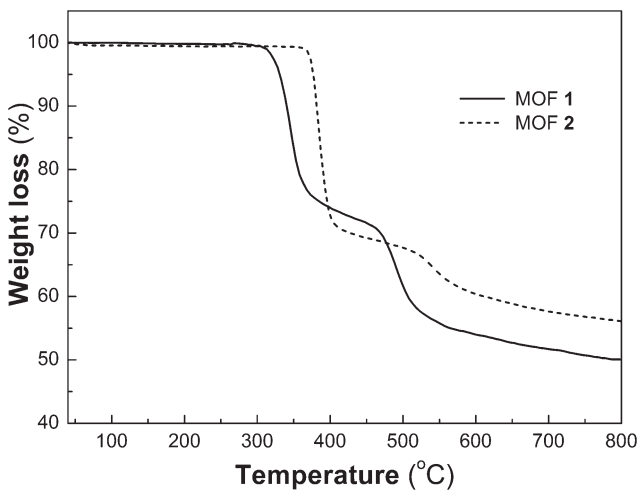

Fig. 6 TGA curves for MOFs **1** and **2**.

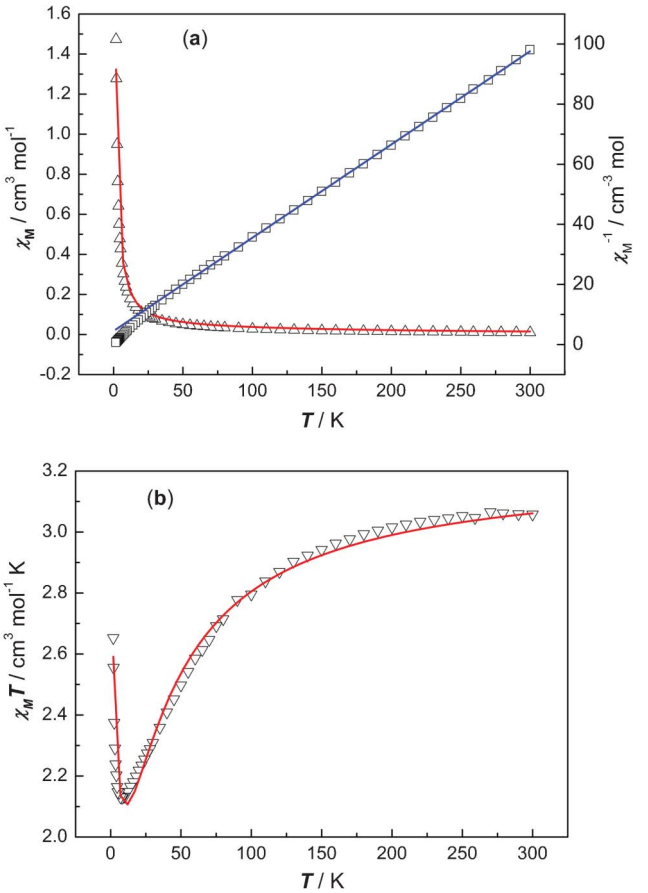

Fig. 7 Temperature dependence of the molar magnetic susceptibility of **1**. (a) The plots of χ_M and χ_M^{-1} *vs.* *T*. (b) The plot of the $\chi_M T$ *vs.* *T*. Solid lines represent the best fitting curves.

Looking at the structure of **1**, the main magnetic interactions may be considered to occur between adjacent Co(II) ions bridged by carboxylic groups in the *syn-anti* conformation mode, whereas the exchange pathways between Co(II) ions bridged through the L ligand can be ignored because of the long Co···Co separation (12.028 Å). However, a detailed quantitative analysis of the susceptibility data for a Co(II) complex is complicated because the orbital moment, spin-orbit coupling, distortions from regular stereochemistry, electron delocalization, and crystal field mixing of excited states into the ground-state affect the magnetic properties in addition to a possible magnetic interaction. Recently, Lloret

et al.[20] have proposed a useful method for analyzing the magnetic data of octahedral high-spin Co(II) compounds that is valid in the condition of weak magnetic coupling as compared to the spin-orbit coupling, $|J/\lambda| < 0.1$. This mothod, unfortunately, is not satisfactory in the present case mainly because the exchange interaction is too weak to show up clearly against the spin-orbit coupling (see below).

In order to estimate the strength of the magnetic coupling in **1**, following a approach reported by Rabu *et al.* for analyzing the magnetic susceptibility of a similar 2D layered Co(II) complex,[19b] we also try to use two exponentials eqn (1) to fit the magnetic data:

$$\chi_M T = 1.99 \times \exp(0.48/T) + 1.23 \times \exp(-42.3/T) \quad (1)$$

where the sum of the two exponential pre-factors equals to the Curie constant, and the first exponential corresponding to the low temperature behaviours is related to the resulting canted moments within the 2D layers, while the second corresponding to the high temperature behaviours stands for the spin-orbit coupling effect. As shown in Fig. 7b, the fit of the present magnetic data using the above expression is quite satisfactory ($R = \sum[(\chi_M T)_{obs} - (\chi_M T)_{calc}]^2/\sum[(\chi_M T)_{obs}]^2 = 8 \times 10^{-4}$). In fact, the variation of the $\chi_M T$ value above 20 K does not correspond to an antiferromagnetic behaviour but to the spin-orbit coupling effect. Therefore, the above eqn (1) adequately describes both the spin-orbit coupling effect that stabilizes discrete levels, and the low temperature divergence of $\chi_M T$ for a 2D ferromagnet as $\exp(4\pi JS^2/T)$.[19b] From the relation $4\pi JS^2 = +0.48$, and assuming the *pseudo*-spin value $S = 1/2$ for the Co(II) ions below 20 K, we deduced the in-plane exchange coupling $J \approx +0.15$ K, which is similar to that reported for a ferromagnetic Co(II) analogue, $J \approx +0.16$ K.[19b] The spin-orbit coupling energy value of −42.3 K is smaller than those reported for other Co(II) derivatives.[19c]

Generally, different Co(II)–O–C–O–Co(II) arrangements can lead to various magnetic interactions between Co(II) ions.[11,21,22] Strongly antiferromagnetic exchange coupling often occurs in the Co(II) complexes with the *syn-syn* carboxylate bridges, weak to moderately antiferromagnetic interactions with the *anti-anti* carboxylate bridges, whereas very weak ferro- or antiferromagnetic coupling can usually be observed in the *syn-anti* carboxylate-bridged Co(II) complexes. In the present work, such a weak ferromagnetic coupling interaction ($J = 0.15$ K) is related to the *syn-anti* carboxylate-bridged Co(II) complexes with a Co···Co distance of 5.462(3) Å. Relevant magneto-structural data for some *syn-anti* carboxylate-bridged Co(II) complexes showing the ferromagnetic interactions are listed in Table 4.[22]

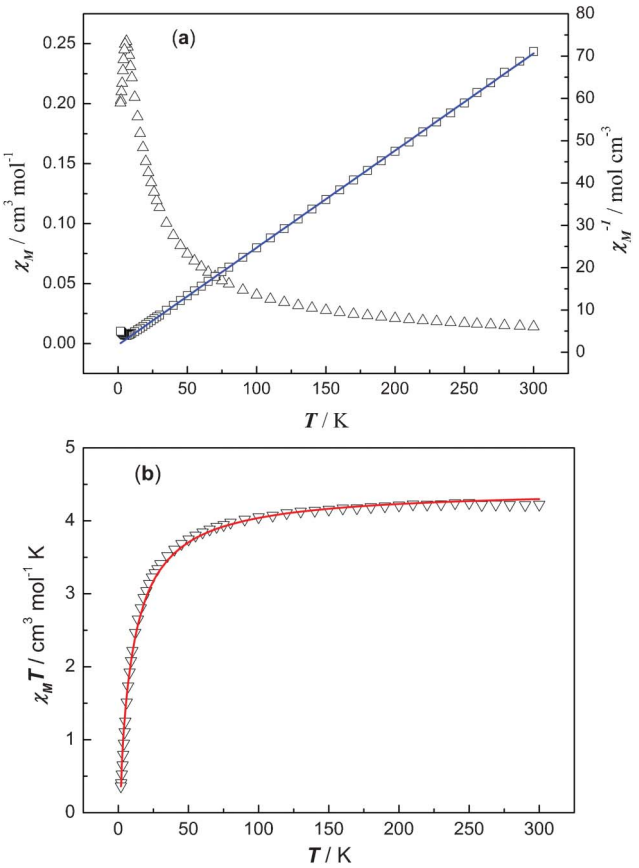

Fig. 8 Temperature dependence of the molar magnetic susceptibility of **2**. (a) The plots of χ_M and χ_M^{-1} *vs.* *T*. (b) The plot of $\chi_M T$ *vs.* *T*. Solid lines represent the best fitting curves.

Magnetic properties of 2

The magnetic susceptibilities of **2** were measured in the temperature range of 1.8–300 K under a 2000 Oe field. The plots of χ_M and χ_M^{-1} *vs.* *T* are shown in Fig. 8a. Upon cooling down, the χ_M value increases to a maximum of 0.25 cm^3 mol^{-1} at *ca.* 6 K and then drops rapidly to 0.2 cm^3 mol^{-1} at 1.8 K. The χ_M^{-1} *vs.* *T* plot is essentially linear, and least-squares fitting of the data to the Curie–Weiss law gave $C = 4.35$ cm^3 K mol^{-1} and $\theta = -7.6$ K. The negative Weiss constant suggests the occurrence

Table 4 Magneto-structural data for some *syn-anti* carboxylate-bridged Co(II) complexes showing the weak ferromagnetic interactions

Complex	Co···Co distance (Å)	J (cm^{-1})	Reference
[Co(L/D-mandelate)(4-MePy)$_3$]$_n$(ClO$_4$)$_n$	5.4648(6)	0.02(7)	22*a*
1	5.462(3)	0.15 K	this work
[Co(L-malate)(H$_2$O)]·2H$_2$O	5.32	0.5 K	22*b*
[Co(phda)(H$_2$O)$_2$]$_n$[a]	5.3164(4)	1.2	22*c*
[Co((S)-citramalate)(H$_2$O)$_2$]	5.23	0.88	22*d*
[Co(O$_2$CCH$_2$OC$_6$H$_5$)$_2$(H$_2$O)$_2$]$_n$	5.09	0.16 K	19*b*
[Co(btx)(BDC)(H$_2$O)]$_n$[b]	4.929	1.43	22*e*
[L^1$_2$Co$_2$(μ-O$_2$CMe)$_2$](BPh$_4$)$_2$[c]	4.797(8)	1.60(2)	22*f*
{[Co(pht)(H$_2$O)(4-bpmp)]·5.5H$_2$O}$_n$[d]	4.54	0.14(3)	22*g*

[a] H$_2$phda = 1,4-phenylenediacetic acid [b] btx = 1,4-bis(1,2,4-triazol-1-ylmethyl)benzene [c] L^1 = 1,3-bis[3-(2-pyridyl)pyrazol-1-yl]propane [d] bpmp = bis(4-pyridylmethyl)piperazine; pht = phthalate.

of antiferromagnetic exchange interactions. The plot of $\chi_M T$ *vs.* T is shown in Fig. 8b. The experimental $\chi_M T$ value at 300 K is about 4.22 cm^3 K mol^{-1}, slightly lower than the spin-only value (4.38 cm^3 K mol^{-1}) for a high-spin Mn(II) ion (S = 5/2, g = 2). Upon cooling, the $\chi_M T$ value decreases smoothly to a value of 3.75 cm^3 K mol^{-1} at 50 K, following sharply to reach a minimum of 0.36 cm^3 K mol^{-1} at 1.8 K. These features also indicate dominant antiferromagnetic coupling between neighboring Mn(II) ions in the 2D layer.

As far as the possibility of the occurrence of a magnetic interaction in **2** concerned, two exchange pathways can be considered: one is the carboxylate group bridge in the *syn-anti* coordination mode; another is through the biphenyl ring of the L ligand. However, the magnetic coupling through the latter exchange pathway should be very weak and can be negligible due to the long Mn···Mn distance (12.079 Å). Thus, from a magnetic point of view, **2** can be regarded as an isolated 1D chain. By use of the well-known expression eqn (2) proposed by Fisher for 1D uniform chains of classical spins:[9,23a]

$$\chi_M = \frac{\chi_{chain}}{1-(2zj'/Ng^2\beta^2)\chi_{chain}}$$
$$\text{where } \chi_{chain} = \frac{Ng^2\beta^2 S(S+1)}{3kT}\frac{1+u}{1-u} \text{ and} \quad (2)$$
$$u = \coth\left[\frac{JS(S+1)}{kT}\right] - \left[\frac{kT}{JS(S+1)}\right]$$

J is based on the spin Hamiltonian $H = -J\sum S_i S_{i+1}$ with S = 5/2, the best fit of the magnetic data of **2** led to g = 2.015(5), J = −0.15(1) cm^{-1}, zJ' = −0.87(3) cm^{-1} ($R = \sum[(\chi_M T)_{obs} - (\chi_M T)_{calc}]^2/\sum[(\chi_M T)_{obs}]^2 = 7 \times 10^{-3}$). The J value is comparable to those reported for other Mn(II) complexes with the *syn-anti* carboxylate bridge, which generally mediates very weak antiferromagnetic interactions.[13a,23]

Conclusions

In summary, by the use of 3,3′-dimethoxy-4,4′-biphenyldicarboxylic acid (H_2L) as a ligand, two novel 3D MOFs $[ML]_n$ (M=Co, **1**; Mn, **2**) have been successfully synthesized under solvothermal conditions. MOF **1** displays a 3D framework with **cds** topology, whereas MOF **2** possesses a doubly interpenetrated 3D α-Po framework. Both **1** and **2** are robust frameworks showing high thermal stability (>310 °C). Magnetic studies demonstrated that the magnetic coupling through the *syn-anti* carboxylate bridge is weak and ferromagnetic between the Co(II) ions in **1**, but weak and antiferromagnetic between the Mn(II) ions in **2**. This work has revealed that utilization of the positioning functional groups as space-filling agents and/or coordination centers may present new opportunities in the design and synthesis of more robust MOFs with tunable properties.

Acknowledgements

Financial support from the National Natural Science Foundation of China (Nos. 21171093 and 20971068) and the State Key Laboratory of Materials-Oriented Chemical Engineering (KL11-03) are gratefully acknowledged.

References

1 (*a*) S. R. Batten and R. Robson, *Angew. Chem., Int. Ed.*, 1998, **37**, 1460; (*b*) B. Moulton and M. J. Zaworotko, *Chem. Rev.*, 2001, **101**, 1629; (*c*) S. Kitagawa and R. Matsuda, *Coord. Chem. Rev.*, 2007, **251**, 2490; (*d*) S. L. James, *Chem. Soc. Rev.*, 2003, **32**, 276; (*e*) C. N. R. Rao, S. Natarajan and R. Vaidhyanathan, *Angew. Chem., Int. Ed.*, 2004, **43**, 1466; (*f*) N. W. Ockwig, O. Delgado-Friederichs, M. O'Keeffe and O. M. Yaghi, *Acc. Chem. Res.*, 2005, **38**, 176.

2 (*a*) J. S. Seo, D. Whang, H. Lee, S. I. Jun, J. Oh, Y. J. Jeon and K. Kim, *Nature*, 2000, **404**, 982; (*b*) O. R. Evans and W. Lin, *Acc. Chem. Res.*, 2002, **35**, 511; (*c*) J. R. Li, R. J. Kuppler and H. C. Zhou, *Chem. Soc. Rev.*, 2009, **38**, 1477; (*d*) B. Chen, S. Xiang and G. Qian, *Acc. Chem. Res.*, 2010, **43**, 1115.

3 (*a*) H. Li, M. Eddaoudi, M. O'Keeffe and O. M. Yaghi, *Nature*, 1999, **402**, 276; (*b*) A. C. Sudik, A. P. Cote and O. M. Yaghi, *Inorg. Chem.*, 2005, **44**, 2998; (*c*) J. H. Cavka, S. Jakobsen, U. Olsbye, N. Guillou, C. Lamberti, S. Bordiga and K. P. Lillerud, *J. Am. Chem. Soc.*, 2008, **130**, 13850.

4 (*a*) S. S. Y. Chui, S. M. F. Lo, J. P. H. Charmant, A. G. Orpen and I. D. Williams, *Science*, 1999, **283**, 1148; (*b*) H. L. Guo, G. S. Zhu, I. J. Hewitt and S. L. Qiu, *J. Am. Chem. Soc.*, 2009, **131**, 1646; (*c*) Y. Qi, F. Luo, Y. X. Che and J. M. Zheng, *Cryst. Growth Des.*, 2008, **8**, 606; (*d*) M. A. Nadeem, D. J. Craig, R. Bircher and J. A. Stride, *Dalton Trans.*, 2010, **39**, 4358.

5 (*a*) L. Pan, H. Liu, X. Lei, X. Huang, D. H. Olson, N. J. Turro and J. Li, *Angew. Chem., Int. Ed.*, 2003, **42**, 542; (*b*) P. S. Mukherjee, N. Das, Y. K. Kryschenko, A. M. Arif and P. J. Stang, *J. Am. Chem. Soc.*, 2004, **126**, 2464; (*c*) H. R. Moon, J. H. Kim and M. P. Suh, *Angew. Chem., Int. Ed.*, 2005, **44**, 1261; (*d*) Q. R. Fang, G. S. Zhu, Z. Jin, M. Xue, X. Wei, D. J. Wang and S. L. Qiu, *Angew. Chem., Int. Ed.*, 2006, **45**, 6126; (*e*) Q. R. Fang, G. S. Zhu, Z. Jin, Y. Y. Ji, J. W. Ye, M. Xue, H. Yang, Y. Wang and S. L. Qiu, *Angew. Chem., Int. Ed.*, 2007, **46**, 6638; (*f*) M. R. Montney, R. M. Supkowski and R. L. LaDuca, *CrystEngComm*, 2008, **10**, 111.

6 (*a*) M. Eddaoudi, J. Kim, N. Rosi, D. Vodak, J. Wachter, M. O'Keeffe and O. M. Yaghi, *Science*, 2002, **295**, 469; (*b*) A. D. Burrows, C. Frost, M. F. Mahon and C. Richardson, *Angew. Chem., Int. Ed.*, 2008, **47**, 8482; (*c*) H. Furukawa, J. Kim, N. W. Ockwig, M. O'Keeffe and O. M. Yaghi, *J. Am. Chem. Soc.*, 2008, **130**, 11650; (*d*) D. J. Lun, G. I. N. Waterhouse and S. G. Telfer, *J. Am. Chem. Soc.*, 2011, **133**, 5806.

7 (*a*) X. Z. Wang, D. R. Zhu, Y. Xu, J. Yang, X. Shen, J. Zhou, N. Fei, X. K. Ke and L. M. Peng, *Cryst. Growth Des.*, 2010, **10**, 887; (*b*) H. J. Zhang, X. Z. Wang, D. R. Zhu, Y. Song, Y. Xu, H. Xu, X. Shen, T. Gao and M. X. Huang, *CrystEngComm*, 2011, **13**, 2586.

8 O. Kahn, *Molecular Magnetism*; VCH, Weinheim, Germany, 1993.

9 G. M. Sheldrick, *Acta Crystallogr., Sect. A: Found. Crystallogr.*, 2008, **A64**, 112.

10 (*a*) Y. H. Zhou and G. L. Zhao, *Acta Crystallogr., Sect. E: Struct. Rep. Online*, 2007, **E63**, m43; (*b*) Z. C. Zhu, S. Karasawa and N. Koga, *Polyhedron*, 2005, **24**, 2102; (*c*) S. Osa, Y. Sunatsuki, Y. Yamamoto, M. Nakamura, T. Shimamoto, N. Matsumoto and N. Re, *Inorg. Chem.*, 2003, **42**, 5507.

11 O. Fabelo, J. Pasán, L. Cañdillas-Delgado, F. S. Delgado, F. Lloret, M. Julve and C. Ruiz-Pérez, *Inorg. Chem.*, 2008, **47**, 8053.

12 (*a*) L. Carlucci, G. Ciani and D. M. Proserpio, *Chem. Commun.*, 2004, 380; (*b*) B. L. Wu, D. Q. Yuan, F. L. Jiang, L. Han, B. Y. Lou, C. P. Liu and M. C. Hong, *Eur. J. Inorg. Chem.*, 2005, 1303; (*c*) G. E. Kostakis, L. Casella, N. Hadjiliadis, E. Monzani, N. Kourkoumelis and J. C. Plakatouras, *Chem. Commun.*, 2005, 3859; (*d*) L. F. Ma, L. Y. Wang, D. H. Lu, S. R. Batten and J. G. Wang, *Cryst. Growth Des.*, 2009, **9**, 1741.

13 (*a*) B. Hachuła, M. Pędras, M. Nowak, J. Kusz, D. Skrzypek, J. Borek and D. Pentak, *J. Coord. Chem.*, 2010, **63**, 67; (*b*) S. H. Zhang and C. Feng, *J. Mol. Struct.*, 2010, **977**, 62.

14 (*a*) M. Xue, G. S. Zhu, Y. X. Li, X. J. Zhao, Z. Jin, E. H. Kang and S. L. Qiu, *Cryst. Growth Des.*, 2008, **8**, 2478; (*b*) H. T. Chung, H. L. Tsai, E. C. Yang, P. H. Chien, C. C. Peng, Y. C. Huang and Y. H. Liu, *Eur. J. Inorg. Chem.*, 2009, 3661.

15 (*a*) G. B. Deacon and R. J. Phillips, *Coord. Chem. Rev.*, 1980, **33**, 227; (*b*) J. P. Costes, F. Dahan and J. P. Laurent, *Inorg.Chem.*, 1985, **24**, 1018; (*c*) S. W. Boettcher, M. H. Bartl, J. G. Hu and G. D. Stucky, *J. Am. Chem. Soc.*, 2005, **127**, 9721; (*d*) V. Robert and G. Lemercier, *J. Am. Chem. Soc.*, 2006, **128**, 1183.

16 L. J. Zhou, Y. Y. Wang, C. H. Zhou, C. J. Wang, Q. Z. Shi and S. M. Peng, *Cryst. Growth Des.*, 2007, **7**, 300.
17 X. L. Wang, Y. Q. Chen, G. C. Liu, H. Y. Lin and J. X. Zhang, *J. Solid State Chem.*, 2009, **182**, 2392.
18 R. L. Carlin, *Magnetochemistry*, Springer-Verlag, Berlin, Heidelberg, 1986.
19 (*a*) J. M. Rueff, N. Masciocchi, P. Rabu, A. Sironi and A. Skoulios, *Eur. J. Inorg. Chem.*, 2001, 2843; (*b*) J. M. Rueff, C. Paulsen, J. Souletie, M. Drillon and P. Rabu, *Solid State Sci.*, 2005, **7**, 431; (*c*) J. M. Rueff, N. Masciocchi, P. Rabu, A. Sironi and A. Skoulios, *Chem.-Eur. J.*, 2002, **8**, 1813.
20 F. Lloret, M. Julve, J. Cano, R. Ruiz-García and E. Pardo, *Inorg. Chim. Acta*, 2008, **361**, 3432.
21 (*a*) F. S. Delgado, M. Hernández-Molina, J. Sanchiz, C. Ruiz-Pérez, Y. Rodríguez-Martín, T. López, F. Lloretd and M. Julved, *CrystEngComm*, 2004, **6**, 106; (*b*) O. Fabelo, L. Cañadillas-Delgado, J. Pasán, F. S. Delgado, F. Lloret, J. Cano, M. Julve and C. Ruiz-Pérez, *Inorg. Chem.*, 2009, **48**, 11342; (*c*) H. Kumagai, Y. Oka, K. Inoue and M. Kurmoo, *J. Chem. Soc., Dalton Trans.*, 2002, 3442; (*d*) E. W. Lee, Y. J. Kim and D. K. Jung, *Inorg. Chem.*, 2002, **41**, 501; (*e*) S. Delgado, J. Sanchiz, C. Ruiz-Pérez, F. Lloret and M. Julve, *Inorg. Chem.*, 2003, **42**, 5938.
22 (*a*) G. Novitchi, G. Pilet and D. Luneau, *Eur. J. Inorg. Chem.*, 2011, 4869; (*b*) A. Beghidja, P. Rabu, G. Rogez and R. Welter, *Chem.–Eur. J.*, 2006, **12**, 7627; (*c*) O. Fabelo, J. Pasán, L. Cañadillas-Delgado, F. Delgado, F. Lloret, M. Julve and C. Ruiz-Pérez, *Inorg. Chem.*, 2009, **48**, 6086; (*d*) A. Beghidja, R. Welter, P. Rabu and G. Rogez, *Inorg. Chim. Acta*, 2007, **360**, 1111; (*e*) X. Xing, X. Song, P. Yang, R. Liu, L. Li and D. Liao, *J. Mol. Struct.*, 2010, **967**, 196; (*f*) V. Mishra, F. Lloret and R. Mukherjee, *Inorg. Chim. Acta*, 2006, **359**, 4053; (*g*) A. Pochodylo, K. Blake, M. Braverman, G. Farnum and R. LaDuca, *Inorg. Chim. Acta*, 2010, **363**, 3951.
23 (*a*) M. E. Fisher, *Am. J. Phys.*, 1964, **32**, 343; (*b*) S. Konar, S. C. Manna, E. Zangrando, T. Mallac, J. Ribas and N. R. Chaudhuri, *Eur. J. Inorg. Chem.*, 2004, 4202; (*c*) J.-Y. Yhang, Y. Ma, A.-L. Cheng, Q. Yue, Q. Sun and E.-Q. Gao, *Dalton Trans.*, 2008, 2061; (*d*) A. Castiñeiras, I. García-Santos and J. M. Varela, *Polyhedron*, 2009, **28**, 860.